LAWRENCE
LIVERMORE
NATIONAL
LABORATORY

LLNL-JRNL-647445

Dynamic Symmetry of Indirectly Driven I. C. F. Capsules on the National Ignition Facility.

R. P. J. Town, D. K. Bradley, A. Kritcher, O. S. Jones, J. R. Rygg, R. Tommasini, M. Barrios, L. R. Benedetti, L. F. Berzak Hopkins, T. Doeppner, E. L. Dewald, D. C. Eder, J. E. Field, S. M. Glenn, N. Izumi, S. W. Haan, S. F. Khan, J. L. Kline, G. A. Kyrala, T. Ma, J. L. Milovich, J. D. Moody, S. R. Nagal, A. E. Pak, J. L. Peterson, H. F. Robey, J. S. Ross, R. H. H. Scott, B. K. Spears, M. J. Edwards, J. D. Kilkenny, O. L. Landen

December 9, 2013

Physics of Plasmas

Disclaimer

Dynamic Symmetry of Indirectly Driven I.C.F. Capsules on the National Ignition Facility*

R. P. J. Town,[1,†] D. K. Bradley,[1] A. Kritcher,[1] O. S. Jones,[1] J. R. Rygg,[1] R. Tommasini,[1] M. Barrios,[1] L. R. Benedetti,[1] L. F. Berzak Hopkins,[1] T. Doeppner,[1] E. L. Dewald,[1] D. C. Eder,[1] J. E. Field,[1] S. M. Glenn,[1] N. Izumi,[1] S. W. Haan,[1] S. F. Khan,[1] J. L. Kline,[2] G. A. Kyrala,[2] T. Ma,[1] J. L. Milovich,[1] J. D. Moody,[1] S. R. Nagel,[1] A. E. Pak,[1] J. L. Peterson,[1] H. F. Robey,[1] J. S. Ross,[1] R. H. H. Scott,[3] B. K. Spears,[1] M. J. Edwards,[1] J. D. Kilkenny,[1] and O. L. Landen[1]

[1]*Lawrence Livermore National Laboratory, P.O. Box 808, Livermore, California 94551-0808, USA*
[2]*Los Alamos National Laboratory, Los Alamos, New Mexico 87545, USA*
[3]*Rutherford Appleton Laboratory, Chilton, Didcot, Oxfordshire, UK*

(Dated: December 2, 2013)

In order to achieve ignition it is important to control the growth of low-mode asymmetries as the capsule is compressed. Understanding the time-dependent evolution of the shape of the imploding capsule, hot spot, and surrounding fuel layer is crucial to optimizing implosion performance. A design and experimental campaign to examine the sources of asymmetry and to measure the symmetry throughout the implosion has been developed and executed on the National Ignition Facility (NIF) [E. I. Moses et al., Phys. Plasmas 16, 041006 (2009)]. For the first time on NIF, two-dimensional radiographs of the capsule during its implosion phase have been measured to infer the symmetry of the radiation drive. Time dependent equatorial symmetry has been measured of gas-filled capsules and capsules with cryogenic THD layers. These measurements have been used to modify the hohlraum geometry and the wavelength tuning to improve the inflight implosion symmetry. We have also expanded our shock timing measurements by the addition of extra mirrors inside the re-entrant cone to allow the simultaneous measurement of shock symmetry in three locations on a single shot, providing a measurement of asymmetries up to mode 4. The shape of the hot spot during final stagnation is measured using time-resolved imaging of the self-emission, and information on the shape of the fuel at stagnation can be obtained from Compton radiography.

I. INTRODUCTION

The primary goal of the National Ignition Campaign (NIC) on the National Ignition Facility (NIF)[1] was to demonstrate fusion ignition and burn. The NIC concentrated on the indirect drive approach to inertial fusion confinement in which a layered DT-filled capsules is placed inside a high-Z hohlraum. The laser beams are incident onto the hohlraum walls and are converted into soft x rays which impinge on the capsule and drive it inwards. By carefully tailoring the laser pulse the x-ray drive can be shaped to compress the DT fuel layer into a cold, high density ($\sim 1000 g/cm^2$) shell surrounding a high temperature ($\sim 10 keV$) lower density hot spot. In order to achieve these conditions it is important that the fuel is maintained on a low adiabat, while converging spherically a factor of about 40.

Haan[2] gave a detailed report of the specification and requirements for the ignition campaign which was summarized in the ignition threshold factor (ITF) formula:

$$ITF = I_0 \left(\frac{M_{DT}}{M_0}\right) \left(\frac{v}{v_0}\right)^8 \left(\frac{\alpha}{\alpha_0}\right)^{-4} \left(1 - 1.2\frac{\Delta R_{HS}}{R_{HS}}\right)^4 \times \left(\frac{M_{clean}}{M_{DT}}\right)^{0.5} (1 - P_{HS}) \quad (1)$$

where I_0 is a scaling multiplier, M_{DT} is the DT fuel mass, v is the implosion velocity, α is the implosion adiabat, ΔR_{HS} is the hot-spot perturbation from average hot-spot radius (R_{HS}), M_{clean} is the clean fuel mass (without mix from the ablator) and P_{HS} is the hot-spot purity factor. The scaling powers of the various terms on the right hand side are a measure of their relative importance to implosion performance. See reference [2] for detailed explanations of the various terms in equation 1. This methodology led to the NIF executing four experimental campaigns (adiabat[3], velocity[4], mix[5], and shape[6]) along with integrated layered implosion experiments[7].

This paper concentrates on the shape experiments and design work that was executed during and after the NIC to control and better understand the implosion symmetry of ignition experiments. The paper is organized as follows: First we review the NIC tuning methodology and discuss the need to measure the fuel shape in section II. The paper reviews the inflight shape measurements in section III, shock symmetry in section IV and the early time symmetry in section V. The inferred symmetry of

*Paper QI3 2, Bull. Am. Phys. Soc. 58, 278 (2013)
†Electronic address: town2@llnl.gov

ignition capsules is discussed in section VI and section VII summarizes the status of the shape campaign.

II. HOTSPOT AND FUEL SHAPE

The shape term in equation 1 is characterized by ΔR_{HS} which is the weighted RMS deviation of the hotspot perimeter radius from its average R_{HS}. Simulations[8] have defined this hotspot region to be the region of the imploded core where the density is less than $max(density)/2$, the $burn\ rate > 0$, and $T_{ion} > 1keV$. For the ignition designs reviewed in [2] the out-of-roundness ($\Delta R_{HS}/R_{HS}$) was expected to be about 13% which would reduce the ITF to 0.5. It was recognized that there was a deficiency in using the hot spot shape to characterize the overall symmetry impact on performance in that this formalism did not account explicitly for the loss in margin that can result from angular modulations in areal density (ρR) of the fuel layer. At the time simulations showed that the variations in ρR were highly correlated with variations in the hot-spot boundary and this deficiency was deemed acceptable.

Experiments cannot directly measure the hotspot perimeter radius, however simulations have found a good correlation between the 17% contour of the x-ray self emission from the imploded core and the hotspot perimeter[6]. Therefore NIF implosion experiments routinely field gated x-ray framing cameras[9] (GXD) to image the time evolution of the x-ray self emission from both the north pole and equatorial region. In addition, image plate detectors surrounding the GXD record the time-integrated self-emission image with different filtration. The hotspot self emission images' 17% contours can be decomposed into Legendre modes (for the equatorial view) and Fourier modes (for the polar view) since the cylindrical hohlraums used on NIF are inherently axisymmetric. For the NIC the requirement for the maximum deviation from round for the two views was set at 10%. This was further divided into a requirement of 7% P2 and 5% P4 distortions (the balance was assigned to higher modes that are increasingly well smoothed by the hohlraum environment).

Symmetry control is achieved by hohlraum geometry and the location and power of the laser beams. As a reminder the NIF's 192 beams are arranged into 48 quads. These quads are further arranged into inner and outer cones. The inner cone consists of eight quads at 23.5° and eight quads at 30° relative to the hohlraum axis of rotation. The outer cone consists of 16 quads at 44.5° and a further 16 quads at 50°. The inherent inner cone fraction (defined as the inner cone power divided by the total power) of the NIF is thus one-third. The initial NIF experiments used scale-544 hohlraums which had a hohlraum diameter of $5440\mu m$ and a length of $10010\mu m$ that was expected to give adequate P2 with the NIF's inherent cone fraction. However, initial experiments showed oblate (or "pancaked") core images that required the use of cross-beam energy transfer (CBET) to transfer energy from the outer cones to the inner cones to achieve a symmetric implosion[10][11][12]. This need for higher cone fraction was explained by the new "high flux" model[13][14] that has been adopted for more recent design work. In 2011 the NIC adopted a new hohlraum geometry (scale-575 with a diameter of $5750\mu m$ and a length of $9425\mu m$) that had more space above the capsule to allow better inner beam propagation and allow symmetry to be achieved at a lower cone fraction with consequent less CBET[4].

Figure 1 shows the self emission image from a 1.5MJ 430TW experiment (N111112) with a wavelength separation of 7.5 Å / 6.0 Å that was still significantly oblate with a P2/P0 of -34% and an RMS variation of 22% despite using the new scale-575 hohlraum. By increasing the wavelength separation to 8.5 Å / 7.3 Å on a subsequent shot (N120412) the self emission image improved substantially with a P2/P0 of -9% and an RMS variation of only 6%, however the yield dropped from 5.7e14 to 1e14. This non-correlation of performance with shape metrics was not unique; figure 2 plots the RMS deviation from round for the equatorial and polar view for all of the layered DT implosion experiments using the scale-575 hohlraum performed from 2011 to 2013. The points are colored coded by the neutron yield for that particular shot. There are a small number of shots that met the ignition requirement to be out of round by less than 10% in each direction (designated by the light blue box) and a rather larger number that met the requirement in one direction. If performance scaled with the hotspot shape metric we would expect to see a strong correlation between yield and hotspot shape asymmetry; In fact there is no such correlation seen in figure 2.

This experimental observation has been confirmed by capsule-only, two-dimensional, cylindrically symmetric geometry simulations using the radiation-hydrodynamics code HYDRA[15]. In an extension of the work presented by Scott[16] a post-shot tuned radiation drive for the NIF layered implosion shot N120205 had various amplitude P2 and P4 flux asymmetries applied during the radiation drive[17]. Figure 3 shows in gray the radiation drive as a function of time. This has been divided into five epochs: the picket, trough, 2nd shock launch, 3rd shock launch and peak. Simulations were undertaken with various amounts of P2 or P4 applied during one of these epochs (the radiation drive was uniform during all other epochs) and then post-processed to generate a range of diagnostics. In particular, the neutron yield, ion temperature and down-scattered ratio (calculated from the neutron spectra) are recorded and the simulated hotspot self-emission images were generated. The blue and green lines for the various epochs and modes represents the applied flux asymmetry to degrade the yield to 50% and 80% respectively. For applied P4 flux asymmetries the yield degrades quickly for asymmetries applied in the peak and trough. For applied P2 flux asymmetries the trough is less important than the peak

and 2nd shock. For both modes the performance degradation for 3rd shock asymmetries is weak. Additional simulations with swings within an epoch, combined P2 and P4 flux asymmetries, and compensating flux asymmetries during different epochs have been performed to build a database of performance metrics with observables. All of these simulations are summarized in figure 4 which shows the simulated yield relative to the symmetric "clean" yield as a function of simulated hot-spot RMS deviation. While there is an overall trend that more distorted hotspot shapes have lower yield there is a large amount of scatter. For example, there are many different scenarios to obtain a RMS deviation of 10% in the hotspot shape that can lead to a large spread in performance from as little as 40% to as much as 95% of the symmetric yield.

As Haan recognized[2] and Scott confirmed in his simulation study[16] it is possible that the hotspot boundary shape is non-conformal with the surrounding cold fuel layer thus breaking the ITF assumption described above. In Scott's case this was achieved by applying a large P4 flux asymmetry early in time that manifests itself in a large oblate hot-spot image which when corrected led to a uniform hotspot, but very non-uniform ρR distribution. Such configurations can also be achieved by time-dependent symmetry swings[17]. By adding the areal density distortion to the hotspot shape we can see that the correlation with yield has improved markedly (Fig. 4 (b)). In particular the low performing simulations that had relatively round hotspot shapes have moved to larger asymmetry because these simulations had large areal density modulations brought about by early time asymmetries.

We are currently developing the Compton radiography technique to measure the dense shell surrounding the hotspot. Encouraging experiments have been performed using the 60-beam OMEGA laser[18] to directly implode a capsule and the short-pulse high intensity OMEGA-EP laser to illuminate a thin gold wire that generated x rays with average photon energies between 60 to 100 keV[19]. Currently NIF is building the advanced radiography capability (ARC)[20] that should deliver 1 kJ/beam in a 10 ps pulse (giving an intensity of $10^{17} W/cm^2$) at 1ω to illuminate a $10\mu m$ diameter gold wire. This is predicted to substantially improve upon the current conventional NIF backlighting capability as shown in Figure 5.

While the correlation with hotspot and areal density is better than with just the hotspot asymmetry there is still some variability for a given asymmetry. This spread can be further reduced by adding a term proportional to the residual non-radial kinetic energy at stagnation as shown in Figure 4 (c). While it is relatively easy to extract this quantity from a simulation we have currently been unable to find a physical observable to monitor experimentally. However remaining residual kinetic energy comes about by symmetry swings throughout the implosion; by controlling symmetry excursions throughout the pulse we should be able to minimize the residual kinetic energy. This has led us to develop a number of new platforms and introduce new ignition requirements on time-dependent symmetry control.

III. INFLIGHT RADIOGRAPHY

Coincident with the development of Compton radiography to image the fuel at stagnation a more conventional backlit imaging technique has been developed[21] to image the imploding capsule inflight from a radius of approximately $300\mu m$ to about $150\mu m$. In this technique two of NIFs 48 quads are redirected from the hohlraum to a germanium foil located $12mm$ from the capsule center in the equatorial plane which generate 10.25 keV Ge $He-\alpha$ x-rays over an approximately $1mm$ diameter spot lasting about $2ns$. To provide a line-of-sight from the Ge backlighter foil through the capsule to the gated x-ray detector, two $0.9 \times 0.83mm$ diagnostic holes are cut out of opposite sides of the hohlraum wall and plugged by high-density carbon windows. A typical frame (from about ten frames obtained on this shot) of the backlit image of an imploding capsule driven in a scale-575 hohlraum is shown in Figure 6 (a). Also shown in Figure 6 (b) is the time-integrated self emission hot-spot image. It is evident from the image that the shell has a diamond shape that is even more pronounced in the self emission image. To be more quantitative the backlit frame is divided into angular sectors, and the radial lineout for each sector is analyzed for the minimum transmission and maximum slope radii. These radii correspond to the peak density of the shell and the ablation surface, respectively. The two contours constructed from these radii of all angular sectors is then fitted to a Legendre polynomial series. By repeating the process for all frames the time evolution of the low mode shape and implosion velocity can be obtained. The time history of the minimum transmission P4 as a function of shell radius (P0) is shown in Figure 7 that shows a large inflight P4 that is growing in time.

The inflight P4 can be reduced by moving the location of the outer cones further away from the equator of the hohlraum. To prevent clipping of the outer cones by the laser entrance hole the hohlraum is lengthened by the same amount as the outer beams move. Detailed integrated hohlraum-capsule simulations using HYDRA showed the presence of an inflight diamond-like P4 that phase inverts to square-like P4 hotspot self-emission image. These calculations show that a hohlraum that is $700\mu m$ longer than the nominal length scale-575 should reduce the inflight P4. A series of experiments with different length hohlraums have been performed[21] that showed a substantial reduction of the inflight P4. Figure 6 (c) shows that the diamond shape P4 has been reduced inflight, but that the hotspot emission has a more pronounced P4 (see 6 (d)) in contradiction to simulations. We believe that the capsule-support tent is impacting the hot-spot images, but is minimally impacting the inflight shape analysis. We have measured the inflight shape of

both symcaps (in which the DT or THD ice fuel layer is replaced by an equivalent mass of plastic) and layered targets. Figure7 shows the time history of P4 for these two target types driven with nominally identical conditions. These inflight shapes are very similar enabling us to tune using the easier-to-field symcap platform rather than the more complex layered capsules. While simulations predicted a reduction in the swing in P4 with the longer hohlraum the experiment does not seem to show this reduction.

IV. SHOCK SYMMETRY

The presence of inflight P4 swings even in the longer hohlraum suggests that we have introduced an asymmetry earlier in the radiation drive. We are examining ways to measure the shell inflight at earlier times, but the required accuracy to diagnose the smaller perturbation at that time and the need for a large uniform area backlighter has led us to extend the shock timing technique to measure the shocks from additional directions. The original NIC shock tuning targets have a deuterium liquid filled ignition capsule with a re-entrant cone that enters through the hohlraum wall to the interior of the capsule to allow a clear optical line of sight on the equator for the VISAR[23] diagnostic to measure the propagating shocks as they break out from the ablator. The interior of the cone near its tip has been modified with two small aluminum mirrors and additional diagnostic holes to provide a view of the pole and 45° in addition to the original straight-through equatorial view (see Figure8a). The first VISAR data obtained in the nominal length scale-575 hohlraum is shown in Figure 8b. The horizontal axis is time and the vertical axis contains the three angular view (each view has multiple fringes thus giving limited spatial information). Lateral motion of the interference fringes is directly proportional to the velocity of the leading shock front. Several discontinuities in the fringes are seen corresponding to the first shock breaking out of the ablator into the liquid deuterium and subsequent shock mergers. The VISAR fringes are lost around the third shock merger on the mirrored channels because of preheat on the aluminum mirror causing a loss of reflectivity (the straight-through equatorial view is unaffected). Later time data could probably be obtained my changing to a beryllium mirror.

Unfolding the VISAR data clearly shows the first shock breaking out from the ablator into the fuel earlier along the 45° line than the pole or equator as shown in Figure 8c. A repeat shot confirmed that this was a geometric effect rather than shot-to-shot variability issue. Using capsule-only HYDRA calculations we estimate the P2 and P4 drive asymmetry on the capsule to be +3.4% and -3.5% respectively during the picket and trough. As expected when we looked at shock symmetry in the $+700\mu m$ longer hohlraum (see Figure 9) the inferred P4 drive asymmetry was reduced to -0.8%, but the P2 drive asymmetry increased to +7%. The increase in P2 is caused by two effects: 1) the outer beams have moved further way from the equator and so provide less drive at the waist in the longer hohlraum and 2) the inner beams have to propagate a longer distance through the hohlraum plasma and thus more energy is absorbed in the plasma volume. The P2 flux asymmetry is easily corrected by increasing the cone fraction in the picket and trough.

V. RE-EMIT

The first shock breakout measurement combines the effect of both the initial picket and the trough of the radiation drive, however simulations have shown that it is possible to introduce symmetry swings by averaging out the asymmetry over these two time periods. Therefore it is important to measure the symmetry of these two epochs independently. The re-emit experiment is designed to look specifically at the picket flux asymmetry during the first $2ns$ of the drive. In this technique[24] the ignition capsule is replaced by a high-Z (typically bismuth) sphere of similar dimensions to the ignition capsule. Two $2.7mm$ diagnostic holes plugged by polyimide windows are cut into the holhraum wall oriented along the line of sight of the gated x-ray detector (GXD) to allow soft x-ray imaging and reduce the background emission from the back-side wall emission. The symmetry of the incoming flux at the capsule is inferred by measuring the soft x-ray re-emission pattern at the limb of the high-Z capsule. By varying the inner cone fraction so the incident P2 flux asymmetry can be adjusted. For the nominal length scale-575 hohlraum a delivered cone fraction of about 36% was predicted to give a symmetric drive. This was confirmed by an experiment without CBET (achieved by setting the inner and outer cones to the same wavelength) shown in Figure 10. Despite the relatively low laser power in the picket the plasma conditions in the laser entrance hole region are cold and dense which is predicted to cause large amounts of CBET with wavelength separation necessary to achieve symmetry in the peak of the pulse (see green dashed line in Figure 10. Consequently the requested incident cone fraction is reduced to 0.14 and CBET boost the cone fraction to required 0.36. To achieve symmetry in the $+700\mu m$ scale-575 hohlraum requires a higher cone fraction than the nominal length scale-575 hohlraum and this has recently been confirmed using the re-emit platform[25].

VI. INFERRED SYMMETRY EVOLUTION

We have measured for the nominal length scale-575 hohlraum the picket, shock, inflight and hotspot self-emission symmetry. We can use these measurements to develop a model of the flux asymmetry on the capsule during the five epochs discussed in section II using the

capsule-only simulation database. Once a combination of flux asymmetries has been found another calculation with these asymmetries throughout the drive is simulated to assess the total impact on performance. The magnitude of the flux asymmetry as a function of time for P2 and P4 is shown in Figure 11. This simulation gave a yield compared to symmetric clean yield of about 50%. The current $+700\mu m$ scale-575 hohlraum has not yet been adequately symmetry tuned and so currently only a modest improvement in performance to about 65% is predicted. Further tuning should reduce the symmetry impact on performance to 10%.

VII. CONCLUSIONS

This paper has reviewed the status of the ignition shape campaign on the NIF. During the NIC the primary measurement of symmetry was the final hotspot self-emission image and the requirement was for the maximum deviation from round for was set at 10%. A number of layered implosion achieved this goal, but there was little correlation between performance and improved shape which suggested that additional measurements were needed. In particular, the shape of the fuel layer has been found to not be as well correlated with the hotspot shape as originally thought.

Simulations have shown that performance is well correlated with hotspot self-emission shape, fuel shape and the remaining residual kinetic energy at stagnation. It is not possible to directly measure the remaining kinetic energy, but by controlling the symmetry swings throughout the implosion the residual kinetic energy can be minimized. This has led us to develop several new diagnostic capabilities to measure and control early time asymmetries. We have applied these techniques to minimize the inflight P4 and P2 and optimize the current ignition hohlraum design.

Acknowledgments

This work performed under the auspices of the U. S. Department of Energy by Lawrence Livermore National Laboratory under Contract No. DE-AC52-07NA27344 and by Los Alamos National Laboratory under Contract No. DE-AC52-06NA25396.

[1] E. Moses, R. Boyd, B. Remington, C. Keane, and R. Al-Ayat, Phys. Plasmas 16, 041006 (2009).

[2] S. W. Haan, J. D. Lindl, D. A. Callahan, D. S. Clark, J. D. Salmonson, B. A. Hammel, L. J. Atherton, R. C. Cook, M. J. Edwards, S. Glenzer, A. V. Hamza, S. P. Hatchett, M. C. Herrmann, D. E. Hinkel, D. D. Ho, H. Huang, O. S. Jones, J. Kline, G. Kyrala, O. L. Landen, B. J. MacGowan, M. M. Marinak, D. D. Meyerhofer, J. L. Milovich, K. A. Moreno, E. I. Moses, D. H. Munro, A. Nikroo, R. E. Olson, K. Peterson, S. M. Pollaine, J. E. Ralph, H. F. Robey, B. K. Spears, P. T. Springer, L. J. Suter, C. A. Thomas, R. P. Town, R. Vesey, S. V. Weber, H. L. Wilkens, and D. C Wilson, Phys. Plasmas. 18, 051001 (2011)

[3] H. F. Robey, T. R. Boehly, P. M. Celliers, J. H. Eggert, D. Hicks, R. F. Smith, G. W. Collins, M. W. Bowers, K. G. Krauter, P. S. Datte, D. H. Munro, J. L. Milovich, O. S. Jones, P. A. Michel, C. A. Thomas, R. E. Olson, S. Pollaine, R. P. J. Town, S. W. Haan, D. A. Callahan, D. Clark, J. Edwards, J. L. Kline, S. Dixit, M. B. Schneider, E. L. Dewald, K. Widmann, J. D. Moody, T. Doeppner, H.B Radousky, A. Throop, D. Kalantar, P. DiNicola, A. Nikroo, J. J. Kroll, A. V. Hamza, J. B. Horner, S. D. Bhandarkar, E. Dzenitis, E. Alger, E. Giraldez, C. Castro, K. Moreno, C. Haynam, K. N. LaFortune, C. Widmayer, M. Shaw, K. Jancaitis, T. Parham, D. M. Holunga, C. F. Walters, B. Haid, E. R. Mapoles, J. Sater, C. R. Gibson, T. Malsbury, J. Fair, D. Trummer, K. R. Coffee, B. Burr, L. V. Berzins, C. Choate, S. J. Brereton, S. Azevedo, H. Chandrasekaran, D. C. Eder, N. D. Masters, A. C. Fisher, P. A. Sterne, B. K. Young, O. L. Landen, B. M. Van Wonterghem, B. J. Macgowan, J. Atherton, J. D. Lindl, D. D. Meyerhofer, E. Moses, Phys. Plasmas. 19, 042706 (2012).

[4] D. A. Callahan, N. B. Meezan, S. H. Glenzer, A. J. MacKinnon, L. R. Benedetti, D. K. Bradley, J. R. Celeste, P. M. Celliers, S. N. Dixit, T. Döppner, E. G. Dzentitis, S. Glenn, S. W. Haan, C. A. Haynam, D. G. Hicks, D. E. Hinkel, O. S. Jones, O. L. Landen, R. A. London, A. G. MacPhee, P. A. Michel, J. D. Moody, J. E. Ralph, H. F. Robey, M. D. Rosen, M. B. Schneider, D. J. Strozzi, L. J. Suter, R. P. J. Town, K. Widmann, E. A. Williams, M. J. Edwards, B. J. Macgowan, J. D. Lindl, L. J. Atherton, G. A. Kyrala, J. L. Kline, R. E. Olson, D. Edgell, S. P. Regan, A. Nikroo, H. Wilkins, J. D. Kilkenny, A. S. Moore, Phys. Plasmas 19, 056305 (2012).

[5] T. Ma, P. K. Patel, N. Izumi, P. T. Springer, M. H. Key, L. J. Atherton, L. R. Benedetti, D. K. Bradley, D. A. Callahan, P. M. Celliers,1C. J. Cerjan, D. S. Clark, E. L. Dewald, S. N. Dixit, T. Doeppner, D. H. Edgell, R. Epstein, S. Glenn, G. Grim, S. W. Haan, B. A. Hammel, D. Hicks, W. W. Hsing, O. S. Jones, S. F. Khan, J. D. Kilkenny,4 J. L. Kline,3 G. A. Kyrala,3 O. L. Landen,1 S. Le Pape,1 B. J. MacGowan,1 A. J. Mackinnon,1 A. G. MacPhee, N. B. Meezan, J. D. Moody, A. Pak, T. Parham, H.-S. Park, J. E. Ralph, S. P. Regan, B. A. Remington, H. F. Robey, J. S. Ross, B. K. Spears, V. Smalyuk, L. J. Suter, R. Tommasini, R. P. Town, S. V. Weber, J. D. Lindl, M. J. Edwards, S. H. Glenzer,1and E. I. Moses, Phys. Rev. Lett. 111, 085004 (2013).

[6] G. A. Kyrala, J. Kline, S. Dixit, S. Glenzer, D. Kalantar, D. Bradley, N. Izumi, N. Meezan, O. Landen, D. Callahan, S. V. Weber, J. P. Holder, S. Glenn, M. J. Edwards, J. Koch, L. J. Suter, S. Haan, R. P. J. Town, P. Michel, O. Jones, S. Langer, J. D. Moody, E . L. Dewald, T. Ma, J. Ralph, A. Hamza, E. Dzenitis, and J. Kilkenny, Phys.

Plasmas 18, 056307 (2011).
[7] M. J. Edwards, P. K. Patel, J. D. Lindl, L. J. Atherton, S. H. Glenzer, S. W. Haan, J. D. Kilkenny, O. L. Landen, E. I. Moses, A. Nikroo, R. Petrasso, T. C. Sangster, P. T. Springer, S. Batha, L. R. Benedetti, L. Bernstein, R. Betti, D. L. Bleuel, T. R. Boehly, D. K. Bradley, J. A. Caggiano, D. A. Callahan, P. M. Celliers, C. J. Cerjan, K. C. Chen, D. S. Clark, G. W. Collins, E. L. Dewald, L. Divol, S. Dixit, T. Doeppner, D. H. Edgell, J. E. Fair, M. Farrell, R. J. Fortner, J. Frenje, M. G. Gatu Johnson, E. Giraldez, V. Yu Glebov, G. Grim, B. A. Hammel, A. V. Hamza, D. R. Harding, S. P. Hatchett, N. Hein, H. W. Herrmann, D. Hicks, D. E. Hinkel, J. P. Hoppe, M and Hsing, W W and Izumi, N and Jacoby, B and Jones, O S and Kalantar, D and Kauffman, R and Kline, J L and Knauer, J. A. Koch, B. J. Kozioziemski, G. Kyrala, K. N. LaFortune, S. Le Pape, R. J. Leeper, R. Lerche, T. Ma, B. J. Macgowan, A. J. MacKinnon, A. MacPhee, E. R. Mapoles, M. M. Marinak, M. Mauldin, P. W. McKenty, N. B. Meezan, P. A. Michel, J. Milovich, J. D. Moody, M. Moran, D. H. Munro, C. L. Olson, K. Opachich, A. E. Pak, T. Parham, H. S. Park, J. E. Ralph, S. P. Regan, B. Remington, H. Rinderknecht, H. F. Robey, M. Rosen, S. Ross, J. D. Salmonson, JJ. Sater, D. H. Schneider, F. H. Seguin, S. M. Sepke, D. A. Shaughnessy, V. A. Smalyuk, B. K. Spears, C. Stoeckl, W. Stoeffl, L. Suter, C. A. Thomas, R. Tommasini, R. P. Town, S. V. Weber, P. J. Wegner, K. Widman, M. Wilke, D. C. Wilson, C. B. Yeamans, and A Zylstra, Phys. Plasmas. 20, 070501 (2013).
[8] D. S. Clark, S. W. Haan, and J. D. Salmonson, Phys. Plasmas 15, 056305 (2008).
[9] J. A. Oertel et al., Rev. Sci. Instrum. 77, 10E308 (2006).
[10] P. Michel, L. Divol, E. A. Williams, S. Weber, C. A. Thomas, D. A. Callahan, S. W. Haan, J. D. Salmonson, S. Dixit, D. E. Hinkel, M. J. Edwards, B. J. MacGowan, J. D. Lindl, S. H. Glenzer, and L. J. Suter, Phys. Rev. Lett. 102, 025004 (2009).
[11] P. Michel, S. H. Glenzer, L. Divol, D. K. Bradley, D. Callahan, S. Dixit, S. Glenn, D. Hinkel, R. K. Kirkwood, J. L. Kline, W. L. Kruer, G. A. Kyrala, S. LePape, N. B. Meezan, R. Town, K. Widmann, E. A. Williams, B. J. MacGowan, J. Lindl, and L. J. Suter, Phys. Plasmas 17, 056305 (2010).
[12] S. H. Glenzer, B. J. MacGowan, P. Michel, N. B. Meezan, L. J. Suter, S. N. Dixit, J. L. Kline, G. A. Kyrala, D. K. Bradley, D. A. Callahan, E. L. Dewald, L. Divol, E. Dzenitis, M. J. Edwards, A. V. Hamza, C. A. Haynam, D. E. Hinkel, D. H. Kalantar, J. D. Kilkenny, O. L. Landen, J. D. Lindl, S. LePape, J. D. Moody, A. Nikroo, T. Parham, M. B. Schneider, R. P. J. Town, P. Wegner, K. Widmann, P. Whitman, B. K. F. Young, B. Van Wonterghem, L. J. Atherton, and E. I. Moses, Science 327, 1228 (2010).
[13] R. P. J. Town, M. D. Rosen, P. A. Michel, L. Divol, J. D. Moody, G. A. Kyrala, M. B. Schneider, J. L. Kline, C. A. Thomas, J. L. Milovich, D. A. Callahan, N. B. Meezan, D. E. Hinkel, E. A. Williams, R. L. Berger, M. J. Edwards, L. J. Suter, S. W. Haan, J. D. Lindl, E. L. Dewald, S. Dixit, S. H. Glenzer, O. L. Landen, E. I. Moses, H. A. Scott, J. A. Harte, and G. B. Zimmerman, Phys. Plasmas 18, 056302, (2011).
[14] M. D. Rosen, H. A. Scott, D. E. Hinkel, E. A. Williams, D. A. Callahan, R. P. J. Town, L. Divol, P. A. Michel, W. L. Kruer, L. J. Suter, R. A. London, J. A. Harte, and G. B. Zimmerman, High Energy Density Phys. 7, 180 (2011).
[15] M. M. Marinak, G. D. Kerbel, N. A. Gentile, O. Jones, D. Munro, S. Pollaine, T. R. Dittrich, and S. W. Haan, Phys. Plasmas 8, 2275 (2001).
[16] R. H. H. Scott, D. S. Clark, D. K. Bradley, D. A. Callahan, M. J. Edwards, S. W. Haan, O. S. Jones, B. K. Spears, M. M. Marinak, R. P. J. Town, P. A. Norreys, and L. J. Suter, Phys. Rev. Lett. 110, 075001 (2013).
[17] A. Kritcher, D. S. Clark, R. P. J. Town, B. K. Spears, S. W. Haan, D. K. Bradley, N04.0004 Bull. Am. Phys. Soc. 58, 193 (2013).
[18] T. R. Boehly, D. L. Brown, R. S. Craxton, R. L. Keck, J. P. Knauer, J. H. Kelly, T. J. Kessler, S. A. Kumpan, S. J. Loucks, S. A. Letzring, F. J. Marshall, R. L. McCrory, S. F. B. Morse, W. Seka, J. M. Soures, C. P. Verdon, Opt. Commun. 133, 495 (1997).
[19] R. Tommasini, S. P. Hatchett, D. S. Hey, C. Iglesias, N. Izumi, J. A. Koch, O. L. Landen, A. J. MacKinnon, C. Sorce, J. A. Delettrez, V. Yu Glebov, T. C. Sangster, and C. Stoeckl, Phys. Plasmas 18, 056309 (2011).
[20] J. K. Crane, G. Tietbohl, P. Arnold, E. S. Bliss, C. Boley, G. Britten, G. Brunton, W. Clark, J. W. Dawson, S. Fochs, R. Hackel, C. Haefner, J. Halpin, J. Heebner, M. Henesian, M. Hermann, J. Hernandez, V. Kanz, B. McHale, J. B. McLeod, H. Nguyen, H. Phan, M. Rushford, B. Shaw, M. Shverdin, R. Sigurdsson, R. Speck, C. Stolz, D. Trummer, J. Wolfe, J. N. Wong, G. C. Siders, and C. P. J. Barty, J. Phys.: Conf. Ser. 244, 032003 (2010).
[21] J. R. Rygg, O. S. Jones, J. E. Field, M. A. Barrios, L. R. Benedetti, G. W. Collins, D. C. Eder, M. J. Edwards, J. L. Kline, J. J. Kroll, O. L. Landen, T. Ma, A. E. Pak, L. Peterson, K. Raman, R. P. J. Town, and D. K. Bradley, submitted to Phys. Rev. Lett. (2013).
[22] S. R. Nagel, J. R¿ Rygg, L. R. Benedetti, T. Ma, M. A. Barrios, S. W. Haan, B. A. Hammel, T. Doeppner, A. E. Pak, R. Tommasini, O. S. Jones, R. P. J. Town, D. K. Bradley, NO4.00012, Bull. Am. Phys. Soc. 58, 195 (2013).
[23] P. M. Celliers, D. K. Bradley, G. W. Collins, D. G. Hicks, T. R. Boehly, and W. J. Armstrong, Rev Sci. Instrum. 75, 4916 (2004).
[24] E. L. Dewald, J. Milovich, C. Thomas, J. Kline, C. Sorce, S. Glenn, and O. L. Landen, Phys. Plasmas 18, 092703 (2011).
[25] A. E. Pak, E. L. Dewald, A. Kritcher, J. Milovich, D. K. Bradley, S. Glenn, O. L. Landen, P. Michel, and R. P. J. Town, JO7.00010 Bull. Am. Phys. Soc. 58, 157 (2013).

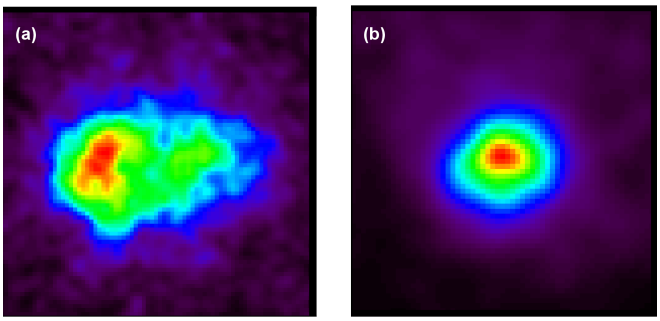

FIG. 1: (Color) The equatorial hotspot self emission for two DT layered implosion experiments with a wavelength separation of (a) 7.5Å / 6.0Å and (b) 8.5Å / 7.3Å between the 23° / 30° inner and outer cones.

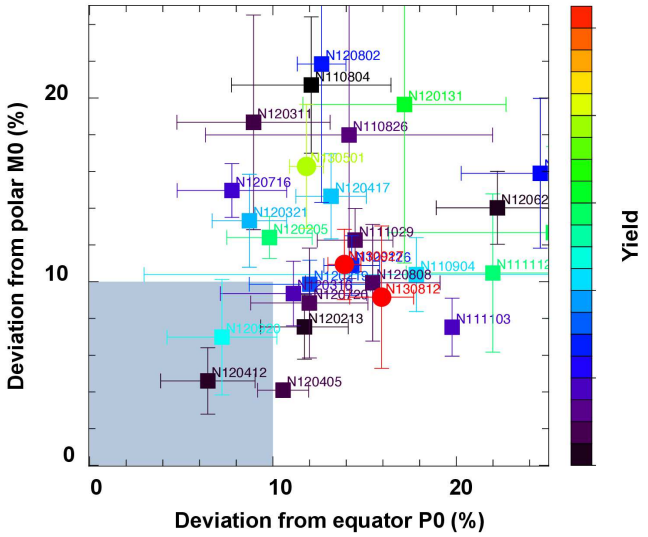

FIG. 2: (Color) The RMS deviation from round from the equator and pole for all layered implosions in scale-575 hohlraum. The 10% out of round requirement is marked by a blue box and the data points are colored by the measured neutron yield. The circle and square correspond to high foot and low foot implosion types. Little neutron yield correlation is seen with asymmetry.

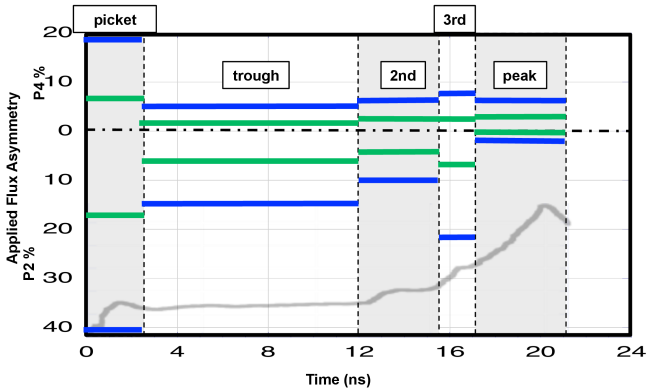

FIG. 3: (Color) The maximum allowed applied P4 and P2 flux asymmetries for various epochs that reduces the simulated yield to 50% (blue) and 80% (green) of symmetric clean yield. The post-shot-tuned radiation drive history is shown in gray.

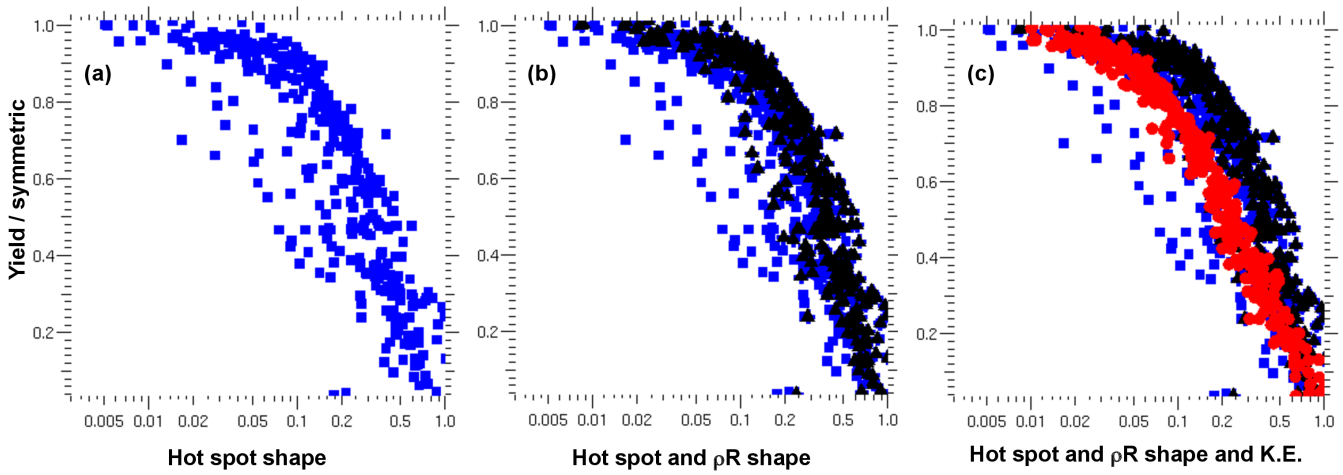

FIG. 4: (Color) The simulated yield compared to the symmetric "clean" yield as a function of RMS deviation from round for (a) the hotspot self emission, (b) the hotspot self emission and the fuel areal density and (c) the hotspot self emission, fuel areal density and residual kinetic energy.

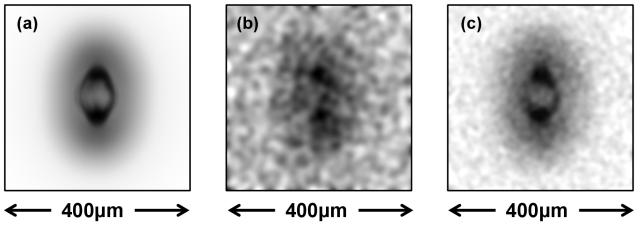

FIG. 5: A comparison of simulated Compton radiographs between (a) a perfect simulated image (b) with a conventional 3ω NIF backlighter at $10^{16} W/cm^2$ incident on a $30\mu m$ gold wire and (c) proposed 1ω ARC at $10^{17} W/cm^2$ incident on a $10\mu m$ wire.

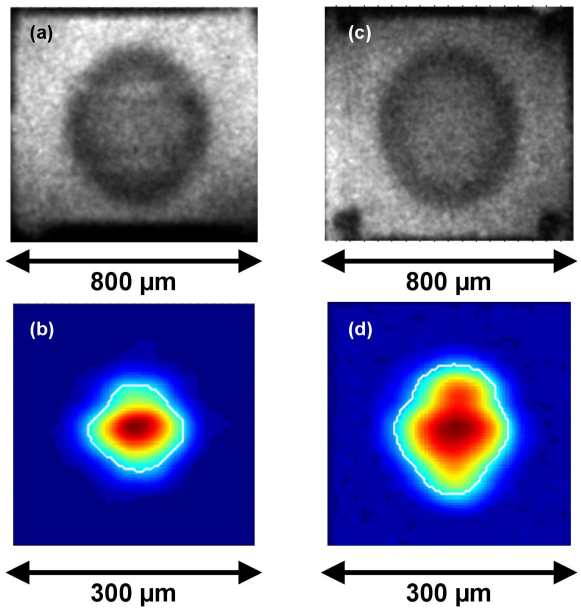

FIG. 6: (Color) Typical (a) backlit 2D radiography image at $220\mu m$ and (b) self emission image of an imploding capsule in a scale-575 hohlraum. Also shown is the (c) backlit image at $220\mu m$ and (d) self emission image when an identical capsule is driven in a $+700\mu m$ scale-575 hohlraum.

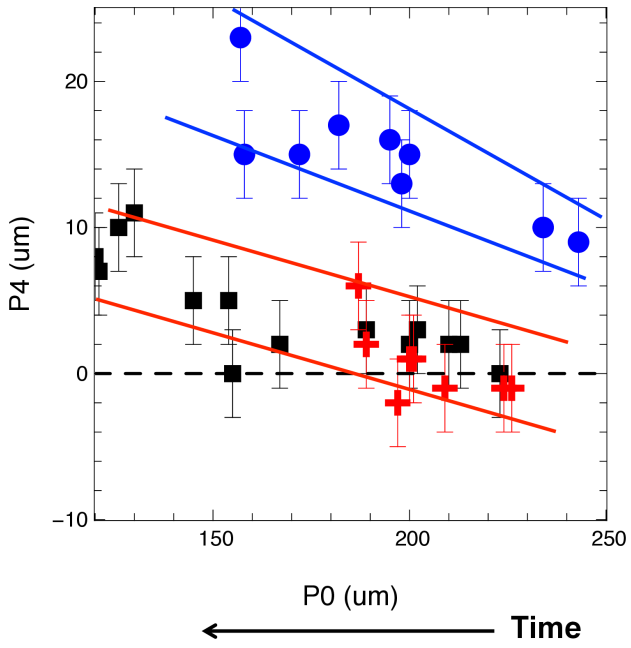

FIG. 7: (Color) The time evolution of the minimum transmission P4 as a function of inflight shell radius (P0) for a symcap in a nominal length scale-575 hohlraum (blue), a symcap (red) and a THD layered capsule (black) in a $+700\mu m$ scale-575 hohlraum.

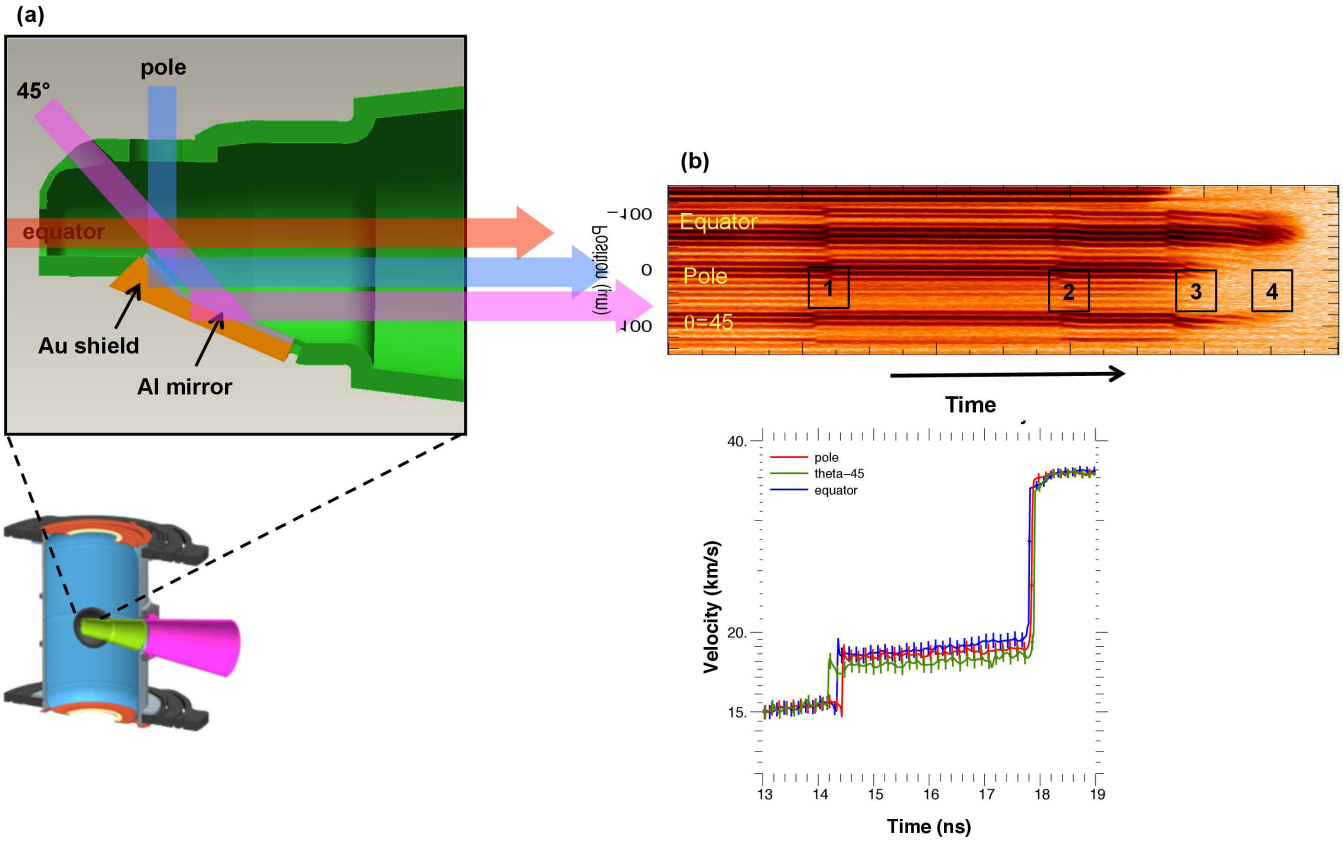

FIG. 8: (Color) (a) The modified re-entrant cone with two additional mirrors and (b) data from the first nominal length scale-575 hohlraum showing that the 45° first shock breakout is earlier than the pole and equator line of sights.

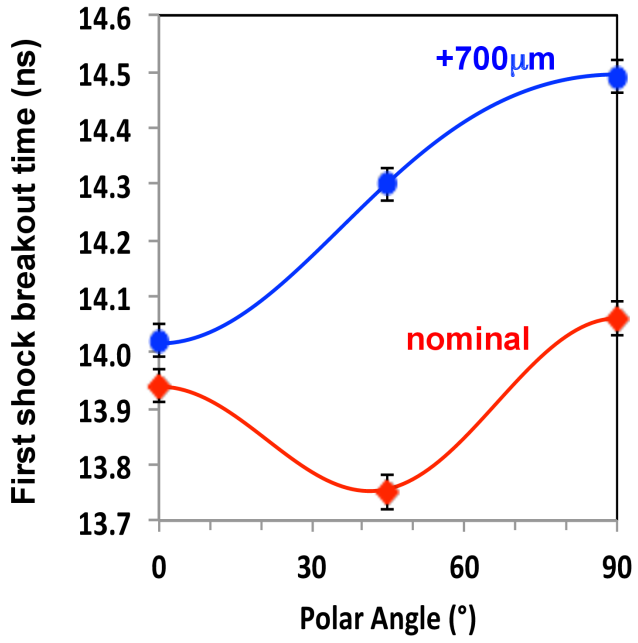

FIG. 9: (Color) The First shock breakout time from the ablator to the liquid deuterium as a function of the three polar angle views for the nominal length in red and the $+700\mu m$ longer in blue scale-575 hohlraum.

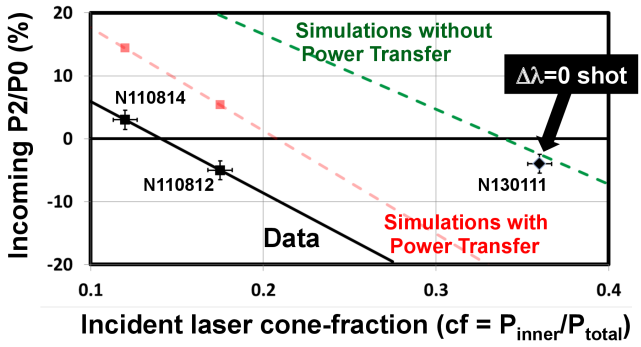

FIG. 10: (Color) Inferred incident P2/P0 at 1.5ns (corresponding to the peak of the picket) as a function of incident laser cone fraction.

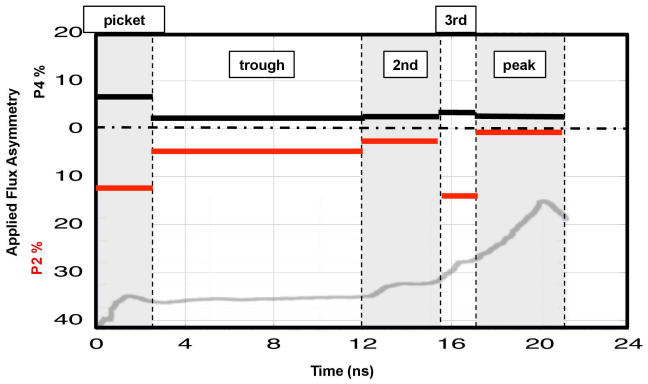

FIG. 11: (Color) The magnitude of applied P4 (black) and P2 (red) flux asymmetry necessary to match the experimental observables for the nominal-length scale-575 hohlraum.